Pressure Effects on the Thermal *Z*/*E* Isomerization of 4-(Dimethylamino)-4′-nitroazobenzene in a Liquid Polymer. A Comparison of Dynamic Solvent Effects in Polymeric and Monomeric Solvents

Akinori Shuto, Toru Takahashi, Yasushi Ohga, Tsutomu Asano, Hirokazu Saito[a], Kohei Matsuo[a], and Hans-Dietrich Lüdemann[b]

Department of Applied Chemistry, Faculty of Engineering, Oita University, Oita 870-1192, Japan
[a] Petroleum Research Laboratory, Research and Development Division, Japan Energy Corporation, Toda 335, Japan
[b] Institut für Biophysik und physikalische Biochemie, Universität Regensburg, 93040 Regensburg

Reprint requests to Prof. T. A.; Fax: +81-97-554-7943, e-mail: asano@cc.oita-u.ac.jp

Z. Naturforsch. **55a,** 616–622 (2000); received January 3, 2000

Effects of pressure on the thermal *Z*/*E* isomerization of 4-(dimethylamino)-4′-nitroazobezene were studied in a silicon oil at various temperatures. The results were compared with the ones previously obtained in glycerol triacetate (GTA) and 2-methylpentane-2,4-diol (MPD).Even in the polymer, pressure effects expected from the transition state theory were obtained at low pressures ($P < 200$ MPa).However, as in GTA and MPD, the transition state theory became invalid at higher pressures. For the polymeric liquid, the macroscopic shear viscosity obviously does not suffice for a quantitative description of the microscopic frictions between the reactant and the solvent molecules.

Key words: High-pressure Kinetics; *Z*/*E* Isomerization; Dynamic Solvent Effects; Liquid Polymer.

Introduction

High pressure has long been recognized as an effective tool to study dynamic routes of fluid reactions. Troe and his co-workers are pioneers in this field [1].Their efforts were mainly concentrated on fast geometrical isomerizations of organic molecules in their electronic excited states and the results are concisely summarized in one of their reviews [2]. We developed our own interests in the field as a result of mechanistic studies of the relatively slow *Z*/*E*-type isomerization about a carbon-nitrogen and a nitrogen-nitrogen double bond in their electronic ground state as shown in the Scheme [3, 4]:

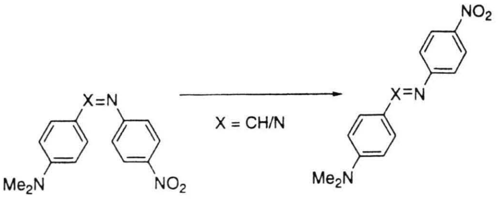

Scheme 1.

The activation volumes were effectively used together with the solvent and the substituent effects in the elucidation of the reaction mechanisms. During the course of the study, pressure-induced retardations that could not be rationalized on the basis of the transition state theory (TST) were discovered in glycerol triacetate (GTA) [5]. In the following investigations [6–9], we did similar measurements also in 2-methylpentane-2,4-diol (MPD) and 2,4-dicyclohexyl-2-methylpentane (DCMP) and concluded that those retardations were dynamic solvent effects. Namely, by applying high external pressure, solvent thermal fluctuations were suppressed and the reactions were shifted from the TST-valid to the TST-invalid condition. The results could be analyzed on the basis of the Sumi-Marcus' version [10, 11] of the two-dimensional reaction coordinate model originally proposed by Agmon and Hopfield (AH model) [12, 13] where the medium and the chemical coordinates are treated independently. In the analysis of the results, the macroscopic shear viscosity of the solvent was used as a measure of the microscopic friction between the reactant and the solvent molecules. In polymer media, however, it is expected that the macroscopic viscosity may not adequately describe the microscopic frictions. In order to examine this possibility, we decided to undertake kinetic pressure-effect measurements on the *Z*/*E* isomerization of 4-(dimethylamino)-4′-nitroazobenzene [(DNAB, X = N in Scheme 1] in a commercially available silicone oil.

0932-0784 / 00 / 0600-0616 $ 06.00 © Verlag der Zeitschrift für Naturforschung, Tübingen · www.znaturforsch.com

Experimental

Material

DNAB [mp 234–235 °C (lit. [14] 232–234 °C)] was a commercial product (Tokyo Kasei Kogyo) and used after recrystallization from toluene. Silicone oil was KF-54 of Shin-Etsu Chemical. The structure and some of the properties are given in Figure 1.

Viscosity Measurements

The high-pressure viscosities of KF-54 were measured by a falling-cylinder viscometer [15] which was calibrated by measuring the falling rate in bis(2-ethylhexyl) sebacate whose viscosity is known [16]. The measurements were performed at 25, 40, 60, 100, and 120 °C. The highest pressure was 427 MPa.

Kinetic Measurements

The unstable *Z*-isomer was formed by irradiation from a xenon flash lamp and its decay was followed spectrophotometrically. The high-pressure vessel with optical windows was essentially the same as described previously [17]. Neither freezing of the solvent nor precipitation of the reactant took place at any of the conditions. It was found that an acidic impurity, probably hydrogen chloride produced in the polymerization reaction between dichlorodimethylsilane and dichlorodiphenylsilane with water, in KF-54 catalyzed the isomerization. In order to suppress this catalysis, piperidine was added to the reaction mixture in the concentration of 1×10^{-3}–10^{-4} mol dm^{-3}. Usually seven measurements were performed at the same condition. The standard deviations of the rate constant were mostly in the range of 0.5–5% depending on the conditions. Because of the lower photo-conversion yield of the *Z*-isomer, the standard deviation became as large as or larger than 10% at the highest pressures.

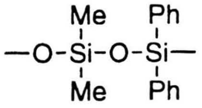

$$-O-\underset{Me}{\overset{Me}{Si}}-O-\underset{Ph}{\overset{Ph}{Si}}-$$

average degree of polymerization:25
mole %: Ph 25, Me 75
kinematic viscosity at 25 °C: 400 cSt

Fig. 1. The structure and some properties of KF-54.

Results and Discussion

Viscosity of KF-54 at High Pressures

Figure 2 illustrates the pressure dependence of the viscosity of KF-54 at various temperatures. The logarithm of the viscosity was linearly correlated with the pressure:

$$\eta = \eta_0 \, e^{\alpha P} . \tag{1}$$

In order to estimate the values of η_0 and α at the reaction temperatures, an empirical correlation between the kinematic viscosity and the temperature (Walther equation) [18] and a linear correlation of α with the logarithm of the kinematic viscosity were used, respectively. The values thus obtained are listed in Table 1.

Table 1. Viscosity Coefficients at 0.1 MPa (η_0/Pa s) and its Pressure Coefficients (α/GPa^{-1}) for KF-54 at Various Temperatures.

T/°C	η_0	α
5	1.17	31.9
15	0.700	29.3
25	0.441	27.0
35	0.289	24.9
40	0.238	23.9

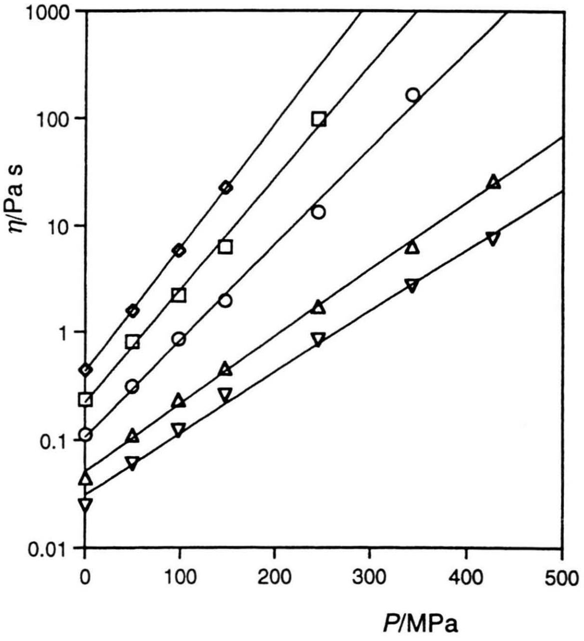

Fig. 2. Pressure dependence of the viscosity of KF-54 at various temperatures. ◇ 25 °C; □ 40 °C; ○ 60 °C; △ 100 °C; ▽ 120 °C.

Isomerization of DNAB in KF-54

The thermal return of the (*Z*)-DNAB to the thermodynamically more stable *E*-isomer followed the first-order rate law at most of the pressures studied. Deviations from the first-order kinetics were noticed at the high end of the pressure range. In this work, however, we restricted ourselves to the pressure range where the reaction followed the first-order decay. The observed rate constants k_{obs} are listed in Table 2, and they are plotted against the pressure P in Fig. 3 together with the k_{obs} in GTA reported earlier [6]. Table 2 also includes the activation volumes at zero pressure and the isobaric activation energies at TST-valid pressures (*vide infra.*). The results in the two solvents were qualitatively the same, i.e., at low pressures, pressure-induced accelerations were observed as in common solvents with low viscosities [19]. However, the pressure effect was reversed at higher pressures. The accelerations were in accordance with a rotation around the nitrogen-nitrogen bond after the heterolytic π-bond cleavage which gives a highly dipolar activated complex **1** [4, 20]. As a result of the stronger solvation in the transition state, the volume of the system decreases ($\Delta V^{\neq} < 0$) in the activation step, and the reaction is accelerated by high external pressure [19]:

$$\left(\frac{\partial \ln k_{obs}}{\partial P}\right)_T = -\frac{\Delta V^{\neq}}{RT}. \tag{2}$$

The faster isomerization in GTA is in accordance with this consideration because the dielectric constant ε of GTA (6.0 at 21 °C) is larger than that of KF-54 (2.88 at 25 °C). The rate constants were even larger in MPD ($\varepsilon = 25.86$ at 20 °C) [7]. The retardations at higher pressures, observed only in highly viscous solvents [6–9], cannot be rationalized on the basis of the TST, however. They must be caused by slow thermal fluctuations of the solvent molecules. In other words, the reaction must have been cast into the TST-invalid viscosity region by high pressure. The shift of the reaction from the TST-valid to the TST-invalid region can be confirmed by comparing the Arrhenius plots at different pressures. At and below 270 MPa, the Arrhenius plots were linear, however clear downward deviations at low temperatures could be seen at and above 360 MPa, as shown in Figure 4. Because of the qualitative similarities of the present results to the ones in GTA and MPD, we decided to analyze the results on the basis of Scheme 2 which was adopted in the previous studies [6–8] as an approximation of

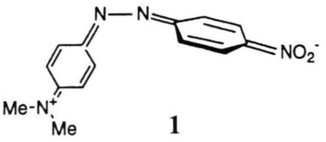

1

Table 2. The Observed (k_{obs}/s^{-1}) and the Fluctuation-Limited (k_f/s^{-1}) Rate Constants together with the Activation Volumes at Zero Pressure ($\Delta V_0^{\neq}/cm^3\ mol^{-1}$) and the Isobaric Activation Energies (Ea/kJ mol^{-1}) for the *Z*/*E* Isomerization of DNAB in KF-54 at Various Temperatures and Pressures.

	5 °C		15 °C		25 °C		35 °C		40 °C		
P/MPa	k_{obs}	k_f	k_{obs}	k_f	k_{obs}	k_f	k_{obs}	k_f	k_{obs}	k_f	Ea
0.1	0.00252		0.00634		0.0154		0.0340		0.0520		62.4
30	0.00296		0.00775		0.0184		0.0410		0.0630		62.8
60	0.00348		0.00920		0.0217		0.0486		0.0746		62.9
90	0.00414		0.0108		0.0254		0.0571		0.0876		62.7
120	0.00479		0.0127		0.0295		0.0667		0.101		62.7
150	0.00559		0.0153		0.0337		0.0766		0.117		62.1
180	0.00647		0.0172		0.0387		0.0880		0.134		62.1
210	0.00751		0.0198		0.0441		0.100		0.153		61.7
240	0.00865		0.0225		0.0503		0.114		0.175		61.6
270	0.00955		0.0257		0.0580		0.129		0.196		61.9
300	0.00913	0.0462	0.0286		0.0651		0.146		0.220		
330	0.00791	0.0201	0.0295	0.302	0.0714	1.79	0.164		0.249		
360	0.00613	0.0104	0.0280	0.118	0.0764	0.806	0.181		0.280		
390	0.00375	0.00481	0.0222	0.0482	0.0748	0.342	0.196		0.300	7.72	
420			0.0153	0.0230	0.0613	0.141	0.195	1.33	0.323	4.44	
450			0.0105	0.0133	0.0402	0.0598	0.173	0.538	0.321	1.88	
480							0.137	0.265	0.284	0.831	
510							0.102	0.150	0.229	0.488	
540									0.172	0.254	
$\Delta V_0^{\neq}$	−13.0		−16.1		−16.0		−16.6		−17.3		

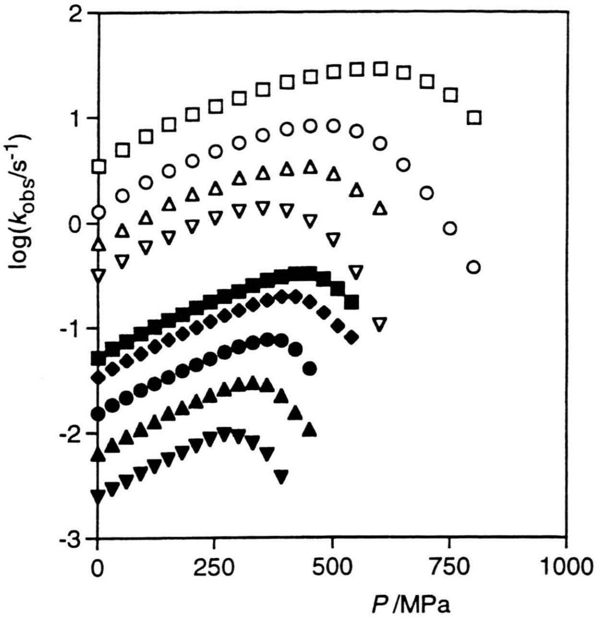

Fig. 3. Pressure effects on the rate of thermal *Z/E* isomerization of DNAB in GTA and KF-54 at various temperatures. □ GTA 40 °C; ○ GTA 25 °C; △ GTA 15 °C; ▽ GTA 5 °C; ■ KF-54 40 °C; ◆ KF-54 35 °C; ● KF-54 25 °C; ▲ KF-54 15 °C; ▼ KF-54 5 °C.

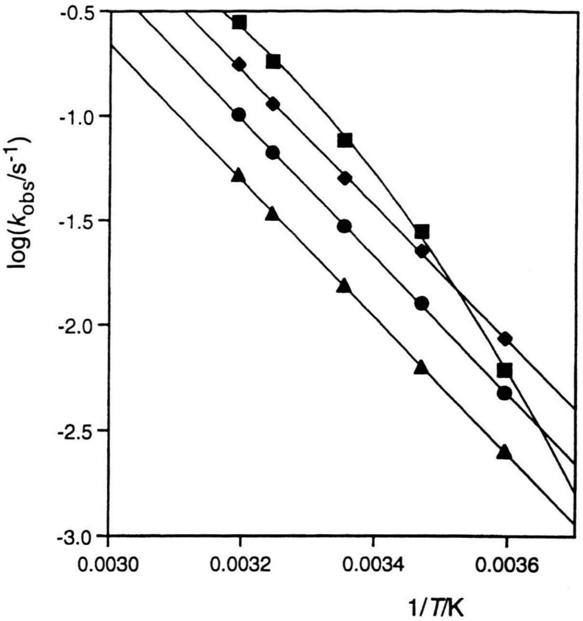

Fig. 4. Arrhenius plots for the *Z/E* isomerization rate of DNAB in KF-54 at various pressures. ■ 360 MPa; ◆ 240 MPa; ● 120 MPa; ▲ 0.1 MPa.

$$\mathrm{Z} \underset{k_{-f}}{\overset{k_f}{\rightleftharpoons}} \mathrm{Z}^* \xrightarrow{k_2} \mathrm{E}$$

Scheme 2.

the AH model. In this scheme, Z and E are the reactant and the product, respectively. The first step describes the solvent reorganization to form solvation spheres that stabilize the activated complex in the second step, where the *Z/E* chemical transformation takes place. Z* describes the reactant molecules in such solvation spheres. By assuming a steady state,

$$\frac{1}{k_{\mathrm{obs}}} = \frac{1}{k_{\mathrm{f}}} + \frac{1}{k_{\mathrm{TST}}} \tag{3}$$

is obtained, where k_{TST} is the rate constant expected from the TST, in other words, the rate constant supposed to be observed when the second step is rate-determining, i.e., $k_{\mathrm{TST}} = k_{\mathrm{f}} k_2 / k_{-\mathrm{f}}$.

The k_{TST} at the TST-invalid pressures can be estimated by extrapolating the pressure dependence of k_{obs} at lower pressures. Several empirical equations have been proposed as functions describing kinetic effects of pressure [17, 21] and one of them,

$$\ln \frac{k_{\mathrm{P}}}{k_{0.1}} = aP + b\ln(1 + cP), \tag{4}$$

was used in this work. k_{P} and $k_{0.1}$ in (4) are the observed rate constants at P and 0.1 MPa, respectively.

The estimated k_{TST} values were put into (3) together with k_{obs} in order to calculate the fluctuation-limited rate constants k_{f}. The k_{f} values thus obtained are also listed in Table 2. As in the monomeric viscous solvents, we could reasonably expect k_{f} to give linear Arrhenius plots because solvent thermal fluctuations require thermal activation. This expectation was met, as shown in Figure 5.

In the reactions of electronically excited molecules, k_{obs} has been found to show an inverse power dependence on the medium viscosity [22]:

$$k_{\mathrm{obs}} = \frac{A}{\eta^{\beta}}, \quad (\beta \le 1). \tag{5}$$

In such reactions, the half-lives were nanoseconds or shorter, and the so-called Kramers' turnover was

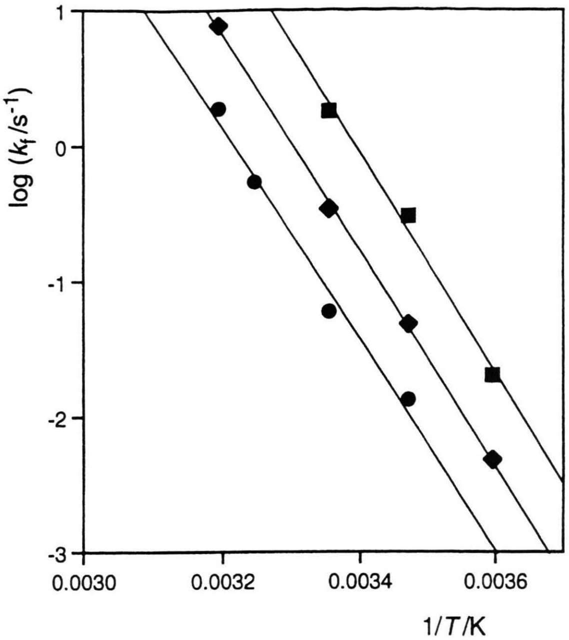

Fig. 5. Arrhenius plots for the fluctuation-limited rate constant in the isomerization of DNAB in KF-54 at several pressures. ■ 330 MPa; ◆ 390 MPa; ● 450 MPa.

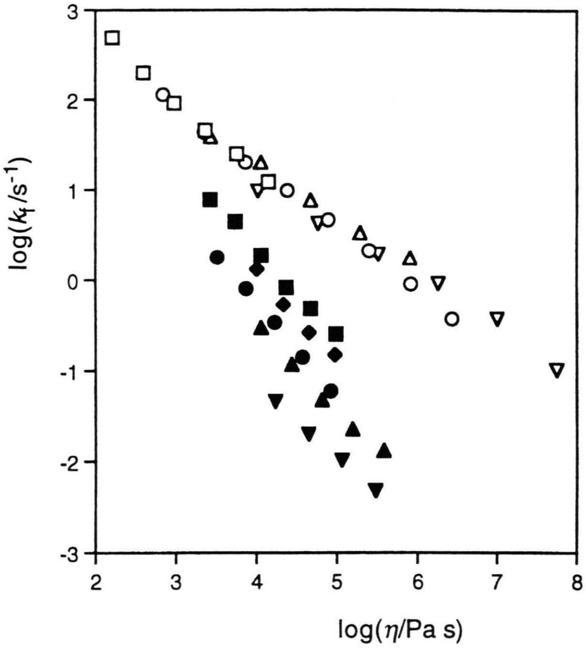

Fig. 6. Viscosity dependence of the fluctuation-limited rate constant in KF-54 and GTA at various temperatures. □ GTA 40 °C; ○ GTA 25 °C; △ GTA 15 °C; ▽ GTA 5 °C; ■ KF-54 40 °C; ◆ KF-54 35 °C; ● KF-54 25 °C; ▲ KF-54 15 °C; ▼ KF-54 5 °C.

observed in compressed gases or in supercritical fluids [2, 22]. Therefore, the reactions must have been fluctuation-limited, i.e., $k_{obs} \approx k_f$, in liquids. This, in turn, suggests a similar viscosity dependence of our k_f. This was in fact observed in GTA and MPD [6, 7]. The log k_f – log η plots found for KF-54 are shown in Figure 6 together with the ones in GTA. As expected, the plots were linear and the slopes were in the range of 0.8–1 [23]. These results imply that our k_f is a rate constant for a process which requires thermal activation, and that the solvent molecules are involved in the process. In other words, Scheme 2 and the two-dimensional reaction-coordinate model that Scheme 2 is based on are valid not only in monomer solvents but also in the present case.

Differences between the Monomeric and the Polymeric Solvents

Although the results in KF-54 look similar to the ones in GTA (Fig. 3), the difference can be seen clearly in the plot of k_f against η (Figure 6). In GTA, the fluctuation-limited rate constant did not show an appreciable temperature dependence at constant viscosity. On the other hand, k_f was clearly dependent on the temperature even at the same viscosity in KF-54. This temperature dependence might be understood by comparing it to the similar results in MPD observed previously [7]. In MPD, the isoviscous temperature dependence was rationalized by assuming that the energy of the system increases in the rearrangement of the solvent molecules. In the initial state the alcohol molecules must be hydrogen-bonded to the lone pair electrons of the nitrogen in the dimethylamino group. In the activated complex **1**, the nitrogen atom is positively charged. Therefore, the solvent molecules have to cleave the hydrogen bonds in the first step to rearrange their dipoles so that the dipolar activated complex is stabilized by the solute-solvent interactions. It is hard to imagine such movements taking place without inducing any structural change in the reactant. Probably the solvent rearrangement and the chemical transformation take place in a partially concerted manner. The detailed analysis based on the Sumi-Marcus model suggested that the energy increase in the first step amounts to ca. 75% of the total activation energy [7]. The same discussion is

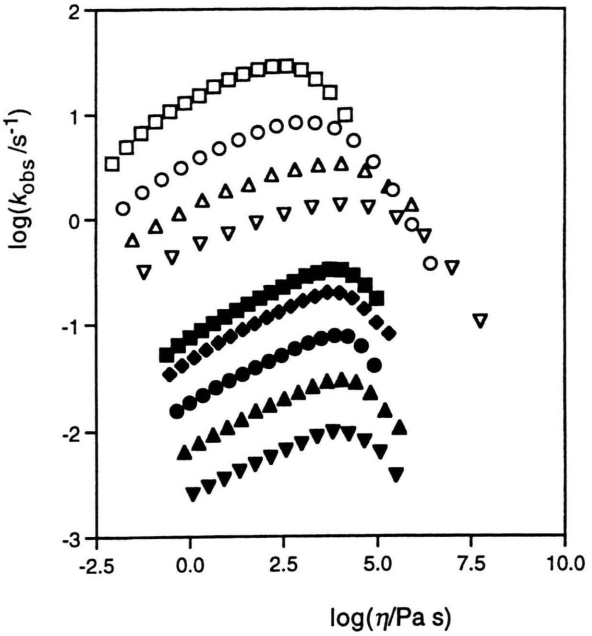

Fig. 7. Viscosity dependence of the *Z/E* isomerization rate of DNAB in GTA and KF-54 at various temperatures.
□ GTA 40 °C; ○ GTA 25 °C; △ GTA 15 °C; ▽ GTA 5 °C; ■ KF-54 40 °C; ◆ KF-54 35 °C; ● KF-54 25 °C; ▲ KF-54 15 °C; ▼ KF-54 5 °C.

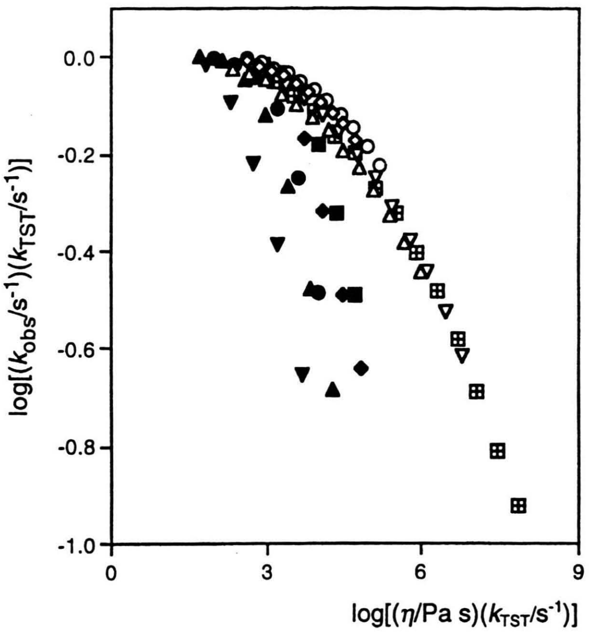

Fig. 8. Dependence of the deviation from TST on the relative time scale of the solvent thermal fluctuation and the chemical conversion.
◇ MPD 35 °C; ○ MPD 25 °C; △ MPD 15 °C; ▽ MPD 5 °C; ⊞ MPD –5 °C; ■ KF-54 40 °C; ◆ KF-54 35 °C; ● KF-54 25 °C; ▲ KF-54 15 °C; ▼ KF-54 5 °C.

difficult to apply to the present system, however. KF-54 molecules do not have hydroxyl groups and are less polar than GTA molecules. If the isoviscous temperature dependence of k_f in KF-54 is caused by the partial concertedness of the chemical and the medium coordinates, we must expect DNAB molecules to behave similarly in GTA, which is not the case, however. The long linear structure of the KF-54 molecules may be responsible for this temperature dependence of k_f. This view is supported by the viscosity dependence of k_{obs} in KF-54. The $\log k_{obs} - \log \eta$ plots are shown in Fig. 7 for GTA and KF-54. In GTA, the viscosity which yields the maximum rate, shifts towards higher values from 10^2 Pa s at 40 °C to 10^4 Pa s at 5 °C. Similar shifts (10^2 Pa s at 35 °C to 10^3 Pa s at –5 °C) were also observed in MPD. In KF-54, on the contrary, the viscosity where k_{obs} is maximal is practically independent of the temperature. The maximum shift in the monomeric solvents can be easily rationalized, i.e., the reaction is accelerated by an increase in temperature, and the larger the rate constant, the faster the solvent fluctuations where the reaction goes into the TST-invalid region. The same must be true in KF-54. However, if there is another factor which does not contribute to η but contributes to the microscopic friction, and if this contribution decreases with increasing temperature, the effect of temperature might be compensated and an almost constant viscosity would be required to make the TST invalid. This assumption of a second microscopic friction and its decrease with increasing temperature in KF-54 is also supported by the plots shown in Figure 8. In this Figure, log (k_{obs}/k_{TST}) is plotted against $\log(\eta \times k_{TST})$ for KF-54 and MPD. The abscissa represents the balance between characteristic times of chemical and the medium coordinates, thus compensating the effect of the reaction rate. The results in GTA were more or less similar to the ones in MPD. Deviations from the TST start at a similar value of $k_{TST} \times \eta$, but k_{obs}/k_{TST} decreases much more rapidly in KF-54 in accordance with the existence of the second friction. Furthermore, the plot for KF-54 rapidly approaches to the ones in MPD with an increase in temperature, a clear indication of a decrease in the second friction. Considering all of these experimental results in Figures 6, 7, and 8, it is reasonable to conclude that in order to describe the microscopic frictions in KF-54, macroscopic shear viscosity is not enough and this, in turn, may be taken to suggest the validity of our assumption that microscopic friction in monomeric liquids can be considered to be proportional to the macroscopic shear viscosity. The second friction in KF-54 might be caused by local segmental rotation of the siloxane chain and/or the rotation of the phenyl side groups. However, a detailed discussion is not possible at this level of our knowledge. Further experiments in polymers with different average chain lengths are in preparation and the results will be reported when completed.

Acknowledgement

Donation of KF-54 by Shin-Etsu Chemical is gratefully acknowledged.

[1] J. Troe, in "High Pressure Chemistry" ed by H. Kelm, Reidel, Dordrecht 1978, pp. 489–520.

[2] J. Schroeder, J. Phys.: Condens. Matter **8**, 9379 (1996).

[3] For the C=N bond isomerization, see T. Asano, H. Furuta, H.-J. Hofmann, R. Cimiraglia, Y. Tsuno, and M. Fujio, J. Org. Chem. **58**, 4418 (1993) and earlier papers cited therein.

[4] For the N=N bond isomerization, see R. Cimiraglia, T. Asano, and H.-J. Hofmann, Gazz. Chim. Ital. **126**, 679 (1996) and earlier papers cited therein.

[5] T. Asano and T. Okada, Chem. Lett. **1987**, 695.

[6] T. Asano, H. Furuta, and H. Sumi, J. Amer. Chem. Soc. **116**, 5545 (1994).

[7] T. Asano, K. Cosstick, H. Furuta, K. Matsuo, and H. Sumi, Bull. Chem. Soc. Japan **69**, 551 (1996).

[8] T. Asano, K. Matsuo, and H. Sumi, Bull. Chem. Soc. Japan **70**, 239 (1997).

[9] Y. Ohga, T. Asano, N. Karger, T. Gross, and H.-D. Lüdemann, Z. Naturforsch. **54a**, 417 (1999).

[10] H. Sumi and R. A. Marcus, J. Chem. Phys. **84**, 4894 (1986).

[11] H. Sumi, J. Phys. Chem., **95**, 3334 (1991).

[12] N. Agmon and J. J. Hopfield, J. Chem. Phys. **78**, 6947 (1983).

[13] N. Agmon and J. J. Hopfield, J. Chem. Phys. **79**, 2042 (1983).

[14] C. L. Bird, J. Soc. Dyers Colour. **70**, 68 (1954).

[15] R. Wolff, T. Nonaka, A. Kubo, and K. Matsuo, Trans. ASME, J. Trib. **114**, 706 (1992).

[16] "ASME Pressure-Viscosity Report", ASME, New York 1953, Vol. II, pp.114–115.

[17] T. Asano and T. Okada, J. Phys. Chem. **88**, 238 (1984).

[18] "Standard Viscosity-Temperature Charts for Liquid Petroleum Products," D341-74, Part 23, Annual Book of ASTM Standards, ASTM, Philadelphia 1985.

[19] The activation volumes in various solvents at various temperatures are listed in: R. van Eldik, T. Asano, and W. J. le Noble, Chem. Rev. **89**, 549 (1989).

[20] The reaction is actually a competition between the nitrogen inversion and the rotation [4] with a major contribution by rotation. Since it had already been shown that the reaction mechanism did not affect the dynamic solvent effect [6–8], no further attempt was made to quantitatively clarify the relative contributions.

[21] C. A. N. Viana and J. C. R. Reis, Pure Appl. Chem. **68**, 1541 (1996).

[22] For a recent review, see A. Drljaca, C. D. Hubbard, R. van Eldik, T. Asano, M. V. Basilevsky, and W. J. le Noble, Chem. Rev. **98**, 2167 (1998).

[23] The β values were 0.98 (40 °C), 0.97 (35 °C), 1.06 (25 °C), 0.90 (15 °C), and 0.78 (5 °C). The value at 25 °C was slightly larger than the theoretically expected highest value, unity. However, we believe that this must be a result of the experimental errors.